# Dynamic Surface Structures and Reactivity of Vanadium-Containing Molybdophosphoric Acid ($H_{3+x}PMo_{12-x}V_xO_{40}$) Keggin Catalysts during Methanol Oxidation and Dehydration

Julie E. Molinari, Lingaiah Nakka,[†] Taejin Kim,[‡] and Israel E. Wachs*

Operando Molecular Spectroscopy and Catalysis Laboratory, Chemical Engineering Department, Lehigh University, Bethlehem, Pennsylvania 18015, United States

S *Supporting Information*

ABSTRACT: The influence of introducing VO_x sites into the primary, bulk structure of molybdenum-containing polyoxometalate $H_{3+x}PMo_{12-x}V_xO_{40}$ ($x = 0, 1, 2, 3$) and secondary, surface structure of supported $VO_x/H_3PMo_{12}O_{40}$ Keggins was investigated to establish their structure−reactivity/selectivity relationships. The resulting Keggins were physically characterized (solid-state ^{51}V NMR and in situ FT-IR, Raman and UV−vis spectroscopy) and chemically probed with CH_3OH (CH_3OH-TPSR spectroscopy and steady-state methanol oxidation/dehydration). The introduction of the VO_x sites into the primary Keggin structure resulted in structural disorder that facilitated decomposition of the Keggins at elevated temperatures and under the corrosive methanol reaction environment. The decomposition was reflected in the expelling of the VO_x units from the primary Keggin structure into the secondary surface VO_x sites where they reacted with surface acidic hydroxyls. For the first time, it was demonstrated that methanol is present as both sorbed species within the Keggin structure as well as surface reactive species during methanol reaction conditions at elevated temperatures ($T < 400\,°C$). Introduction of the VO_x sites increased the formaldehyde selectivity and decreased the dimethyl ether selectivity. The VO_x units in the primary Keggin structure were slightly more active than the surface VO_x species, and both VO_x sites were significantly more active than the MoO_x sites in the primary Keggin structure. The relatively constant TOF_{redox} values with number of VO_x sites in the Keggin reflect that only one VO_x site is involved in methanol oxidation to formaldehyde. Although introducing VO_x into the Keggin decreased the UV−vis edge energy (Eg) and increased the TOF_{redox} relative to the V-free $H_3PMo_{12}O_{40}$ Keggin, a direct relationship between TOF_{redox} and Eg was not found to be present for the $H_3PMo_{12-x}V_xO_{40}$ Keggins. These new fundamental insights demonstrate the importance of performing in situ molecular spectroscopy characterization studies under reaction conditions and reveal that the Keggin structures are dynamic and should not be assumed to be ideal, static model catalytic structures.
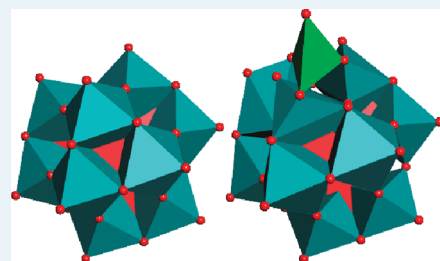
KEYWORDS: catalysts, heteropolyoxo anions, heteropoly acids, HPAs, polyoxometalates, POMs, molybdophosphoric acid, MPA, molybdenum oxide, vanadium oxide, reaction, CH_3OH, oxidation, HCHO, formaldehyde, dehydration, dimethyl ether, DME, Spectroscopy, Raman, IR, UV−vis, in situ, TPSR, ^{51}V NMR, TPSR, ambient

■ INTRODUCTION

Molybdenum-based Keggin polyoxometalates (POMs) containing vanadium, with the formula $H_{3+x}PMo_{12-x}V_xO_{40}$ (MPAV) and x varying from 0 to 3, exhibit unique catalytic properties because of their bifunctional nature and have been investigated as catalysts both for acidic and for oxidative reactions.[1−3] The addition of vanadium centers are beneficial for redox catalysis, shifting the molybdophosphoric acid (MPA) reactivity from acidic to redox character as evidenced by the shift in selectivity of the methanol oxidation reaction from formation of CH_3OCH_3 (DME) to HCHO, respectively.[4] The addition of vanadium to the molybdenum-based POMs also affects the reactivity toward methanol oxidation/dehydration with the maximum activity attained for MPAV2[5,6] and substitution of more vanadium causing a decrease in reactivity.[4] This catalytic observation was rationalized by concluding that the MPAV Keggin structure can only tolerate one or two vanadium cation(s) per Keggin unit since higher vanadium contents destabilize the crystalline MPA molecular structure.[7]

Recent in situ characterization studies by EPR, UV−vis, Raman, FTIR, and NMR during heat treatment up to 350 °C have revealed that the vanadium cation can be expelled from the MPAV Keggin.[8−10] Even when the vanadium cation is in the primary structure after synthesis, it can migrate to the secondary structure as a surface vanadyl group under reaction conditions.[11] The migration of vanadium from the primary Keggin structure to the secondary cationic position depends on the content of vanadium, treatment temperature, and reactive environments.[8,12,13] Furthermore, the MPAV Keggin structure can also decompose at elevated temperatures and in certain reaction environments. In situ UV−vis spectroscopic characterization during methanol oxidation, $O_2/CH_3OH = 10/1, 3/1$, and $0.5/1$, revealed that the MPAV Keggin structure decomposes at

$\sim$400 °C with resultant loss in catalytic activity and selectivity.[12] During propylene oxidation by MPAV Keggins, in situ X-ray diffraction (XRD) and X-ray absorption spectroscopy (XAS) characterization studies indicated partial decomposition of the Keggin takes place at reaction temperatures up to $\sim$350 °C.[13] In situ transmission electron microscopy (TEM) studies of the MPA Keggin have directly observed MoO_x expulsion and structural rearrangement to a twinned structure from thermal treatment at elevated temperatures.[14] This structural transformation, however, may possibly have also been induced by electron beam damage and additional in situ TEM studies are necessary to resolve this possibility.

It has also been suggested that an intermediate "ill-defined" MoO_3-type mixed oxide species resulting from the partial decomposition of molybdena and vanadia Keggins might possibly be the active species under industrial partial oxidation conditions.[15] In situ Raman spectroscopy experiments during thermal treatment and under propylene oxidation conditions have revealed that the decomposition of the intact Keggin anions begins with expulsion of vanadyl and molybdenyl species forming defective Keggin stuctures, and then follows with the disintegration of the defective Keggin unit to intermediate MoO_x species before finally fully decomposing to MoO_3.[15] The appearance of a number "multiplet" of Raman bands in the 900$-$1000 cm^{-1} spectral region appears to be indicative of the transformation of intact Keggin anions to the intermediate mixed MoO_x phase.[15] In addition to structural changes of the MPAV Keggins at elevated temperatures and reaction conditions, the Mo and V cations can also change their oxidation states. During isobutane oxidation by $H_4PMo_{11}V_1O_{40}$, in situ electron paramagnetic resonance (EPR) spectroscopy showed that none of the cations are reduced at reaction temperatures below 300 °C.[7] During isobutane oxidation at 350 °C, however, $\sim$32% of the V cations become reduced to V^{4+} and the Mo cations remain fully oxidized as Mo^{6+}. Almost compete reduction of the V^{5+} cations to V^{4+} cations was observed during the more reducing methanol oxidation reaction at 300 °C using 2% CH_3OH/He in the absence of oxygen.[3,5,16]

The above literature summary of oxidation reactions by MPAV Keggins reveals the complexity of these catalysts and the need for in situ characterization studies, especially in situ Raman characterization studies under reaction conditions because of sensitivity of Raman spectroscopy to molecular structure, to fully understand their structure$-$activity/selectivity relationships. The above literature summary also reveals the lack of information regarding the effect of the expelled vanadia species on MPA Keggin reactivity. In the present paper, a series of vanadium incorporated MPA Keggins, where vanadium is introduced into both the primary and the secondary Keggin structure, are examined for the first time with in situ Raman spectroscopy during methanol oxidation to determine their molecular structural evolution under reaction conditions. Deliberate deposition of a vanadia surface species onto the secondary structure of the intact MPA Keggin was employed to establish the role of the expelled vanadia species during partial methanol oxidation conditions. In addition, MPAV Keggins at varying levels of vanadium incorporation were characterized by in situ Raman spectroscopy during partial methanol oxidation under typical reaction condition to establish a relationship between activity and Keggin structure, bulk/surface properties, level of decomposition, and extent of vanadia expulsion. The Raman characterization is complemented by solid state ^{51}V NMR spectroscopy under

ambient conditions and in situ UV$-$vis and IR spectroscopy. The new fundamental insights from these studies confirm the dynamic nature of both the bulk and the surface structures of the MPAV Keggins under methanol oxidation/dehydration conditions and their structure$-$activity/selectivity relationships.

■ EXPERIMENTAL SECTION

Catalysts. The $H_3PMo_{12}O_{40}$ and $H_{3+x}PMo_{12-x}V_xO_{40}$ (x = 1,2,3) catalysts were purchased from Aldrich Chemical Co. and Nippon Inorganic Color and Chemical Co., respectively. The vanadium-containing molybdophosphoric acid catalysts, $H_{3+x}PMo_{12-x}V_xO_{40}$ (x = 1, 2, 3), are denoted as MPAV1, MPAV2, and MPAV3, respectively. In addition, vanadia was also introduced onto the surface or secondary structure of MPA.[17] An aqueous solution containing an appropriate amount of VO^{2+} ions was prepared by reaction of crystalline V_2O_5 with oxalic acid at about 100 °C by keeping VO^{2+}/MPA molar ratio equal to 1.5. After complete dissolution of the V_2O_5 solid, the solution was cooled to room temperature, and the required amount of MPA was added. The excess water was then removed by evaporation at 100 °C, and the dried mass was subsequently calcined at 300 °C in air for 3 h. This catalyst is denoted as VOMPA (vanadia on MPA).

Solid-State ^{51}V NMR Spectroscopy. The solid-state ^{51}V NMR spectra were recorded under ambient conditions with a General Electric Model GN-300 NMR spectrometer at 78.93 MHz to determine the structural integrity of the samples. The instrument was equipped with a Nicolet 2090-IIIA high-speed digital oscilloscope and a 7 mm MAS NMR Doty Scientific probe. The measurements were carried out on spinning samples with a simple one-pulse excitation of 1 μs width, a preacquisition delay of 10 μs, a dwell time of 0.5 μs, and a relaxation delay of 5$-$10 s. The NMR spectra were obtained by accumulation of 3840 scans for each sample. Prior to Fourier transformation, the signal-averaged free induction decays were multiplied by an exponential function equivalent to 500 Hz line broadening to decrease noise in the spectra. All chemical shifts were referenced against the $VOCl_3$ liquid standard.

In Situ Raman Spectroscopy. The in situ Raman spectra of the HPAs were collected with a Horiba-Jobin Yvon LabRam-HR spectrometer equipped with a confocal microscope, 2400/900 grooves/mm gratings, and a notch filter. The laser excitation at 532 nm (visible/green) was supplied by a Yag double diode pumped laser (20 mW). The scattered photons were directed and focused onto a single-stage monochromator and measured with a UV-sensitive LN_2-cooled CCD detector (Horiba-Jobin Yvon CCD-3000 V). The powdered samples, $\sim$5$-$10 mg, were loosely spread onto a small ceramic sample holder inside the environmental cell (Linkam T-1500) and placed below the confocal microscope. The dehydration of the samples was carried out by heating the environmental cell at different temperatures under O_2/He flow (30 mL/min). After reaching the desired temperature, the samples were dehydrated for 30 min before recording the Raman spectrum. Methanol oxidation/dehydration reaction studies in flowing 6% CH_3OH/13% O_2/balance He (30 mL/min) were subsequently performed at different temperatures.

In Situ FT-IR Spectroscopy. The in situ IR spectra of catalyst samples under ambient, dehydrated, and after methanol chemisorption were obtained using a Thermo Nicolet 8700 spectrometer equipped with a DTGS detector. The Thermo Nicolet 8700 was modified to incorporate the Harrick Praying Mantis Attachment (model DRA-2) for diffuse reflectance spectroscopy.

The diffuse reflectance experimental setup within the Thermo Nicolet 8700 computer program Omnic was set to calculate log(1/reflectance) versus wavenumber. Since transmittance and reflectance are mathematically identical, and therefore log(1/reflectance) and the units of absorbance are equivalent, the Omnic software package uses log(1/reflectance) and absorbance interchangeably. Spectra are plotted in units of absorbance versus wavenumber. Approximately 30 mg of each finely ground sample was loaded into the cup of the Harrick Cell (model HVC-DR2 with high pressure dome). For dehydration, the samples were treated at 250 °C with O_2/Ar at a flow rate of 30 mL/min for ~1 h to remove any possible adsorbed impurities and moisture, and then lowered to 110 °C. For collection of in situ IR spectra, the dehydrated catalyst samples were exposed to a continuously flowing Ar environment for another 1 h at 100 °C to remove any physically adsorbed oxygen or potential background gases. Methanol was then chemisorbed by replacing the Ar flow with a CH_3OH/He gas mixture (2000 ppm methanol; 30 mL/min) at 100 °C for 30 min. The IR spectra were recorded at a resolution of 4 cm^{-1} using 72 signal averaged scans.

In Situ UV–vis Diffuse Reflectance Spectroscopy (DRS). Solid catalyst samples were examined using a Varian Cary 5E UV–vis spectrophotometer equipped with the Harrick Praying Mantis Attachment (model DRA-2) for diffuse reflectance spectroscopy. The reference beam was passed through a 1.5 absorbance unit filter to minimize background noise. Approximately 30 mg of each finely ground sample was loaded into the cup of the Harrick Cell (model HVC-DR2 with high pressure dome). A magnesium oxide white reflectance standard baseline was collected under ambient conditions. Magnesium oxide was also physically mixed (50/50 w/w) with the samples to increase sample reflectivity. The Cary 5 computer program parameters were set to calculate and plot absorbance versus wavelength. The spectrum of each catalyst sample was collected over the wavelength range of 200–800 nm under ambient conditions. Bulk V_2O_5 was also examined as a V(V) reference standard. For collection of in situ UV–vis spectra of the dehydrated catalysts, the samples were treated at 230 °C for 1 h under flowing 10%O_2/Ar at a flow rate of 30 mL/min. For collection of in situ UV–vis spectra during methanol oxidation, the dehydrated catalysts were treated with flowing O_2/CH_3OH/Ar for 30 min by using a combined flow of 10% O_2/Ar at 15 mL/min and 2000 ppm CH_3OH/He at 15 mL/min. The UV–vis DRS spectra were analyzed using the Kubelka–Munk function $F(R_\infty)$ and evaluated for the band gap value (E_g) using the method of Davis and Mott[18] for vanadium oxides as further described by Gao[19] and for molybdenum oxides as further described by Tian.[20]

CH_3OH-Temperature Programmed Surface Reaction (TPSR) Spectroscopy. The CH_3OH-TPSR spectroscopy measurements were performed on an Altamira (AMI-200) system equipped with an online quadrupole mass spectrometer (Dycor Dymaxion DME200MS). About 200 mg of catalyst was typically loaded into a U-shaped quartz tube and initially treated at 250 °C (Ultra Zero grade O_2/He, 30 mL/min) for ~1 h to remove any possible adsorbed impurities and moisture. To ensure that the catalysts remained in a fully oxidized state, the pretreated catalyst samples were first cooled down in flowing air to 110 °C and then switched to an ultra high pure He flow with further cooling to 100 °C. After flushing with continuously flowing He for another 1 h at 100 °C to remove any physically adsorbed oxygen or potential background gases, a CH_3OH/He gas mixture (2000 ppm methanol) feed was introduced at 30 mL/min for CH_3OH

chemisorption and maintained for ~40 min. Previous work demonstrated that the adsorption temperature of 100 °C significantly minimizes the presence of physically adsorbed methanol on the samples since physically adsorbed CH_3OH desorbs below this temperature.[21,22] After methanol adsorption, the MPAV POM catalysts were again purged at 100 °C with ultra high purity (UHP) He for an additional 1 h to remove any residual physically adsorbed methanol. The CH_3OH-TPSR spectroscopy experiment was then performed with a heating rate of 10 °C/min in the flowing UHP He, and desorption products were monitored with the online MS. The m/e values used to detect the different desorption products were CH_3OH (m/e = 31), H_2CO (m/e = 30), CH_3OCH_3-DME (m/e = 45), $(CH_3O)_2CH_2$-DMM (m/e = 76), CO_2 (m/e = 44), and CO (m/e = 28). For desorbing products that gave rise to several fragments in the mass spectrometer, additional m/e values were also collected to confirm the identity of the desorbing products (e.g., m/e = 45 for $CH_3OCH_3^+$ and m/e = 15 for the associated CH_3^+ cracking fragment).

CH_3OH Oxidation. The steady-state methanol oxidation studies were performed in an isothermal fixed-bed reactor at atmospheric pressure operating under differential reaction conditions. In a typical experiment, about 30 mg of catalyst was held in between two glass wool beds and pretreated under O_2/He flow at 250 °C for 30 min before passing the gaseous reactants at the desired reaction temperature. The volume composition of the gaseous reactant feed was 6% CH_3OH, 13% O_2 and balance He, with a total flow rate of ~100 mL/min. The methanol conversion and reaction products were analyzed using an online gas chromatograph (HP 5890 series II) equipped with TCD and FID detectors. A Carboxene-1000 packed column and a CP-sil 5CB capillary column were used in parallel for TCD and FID, respectively. The number of exposed redox sites per gram, Ns, for the V-free MPA sample was taken to be 12 sites per Keggin for each Mo atom, adjusted as per the molecular mass. The number of exposed redox sites per gram, Ns, of each V-containing MPAV catalyst was determined from the respective number of vanadium sites present in each Keggin molecule (1 V site for MPAV1, 2 V sites for MPAV2, etc.) and adjusted as per the molecular mass. Since the remaining Mo sites in the V-containing MPAV Keggins (11 for MPAV1, 10 for MPAV2, etc.) also contribute to minor redox activity, the residual contribution from the Mo-based redox sites has been calculated and subtracted out. In the case of VOMPA, an average of 1.5 V sites per Keggin molecule was used and adjusted as per the molecular mass to determine Ns per gram. 1.5 V sites were chosen for VOMPA since the VOMPA synthesis procedure was designed so that, stoichiometrically, 1.5 vanadia groups were deposited per Keggin. Residual Mo-based redox activity for VOMPA was calculated as per 10.5 (average) remaining Mo sites, and subtracted out. Please note that the MPA Ns and TOF calculations are for Mo-based redox activity, and the V-containing MPAV and VOMPA Ns and TOF calculations are for V-based redox activity only. The catalytic turnover frequencies (TOF) for methanol oxidation to redox products (HCHO, MF, and DMM) were determined by normalizing the steady-state reaction rates per gram by the number of redox sites per gram of catalyst (Ns).
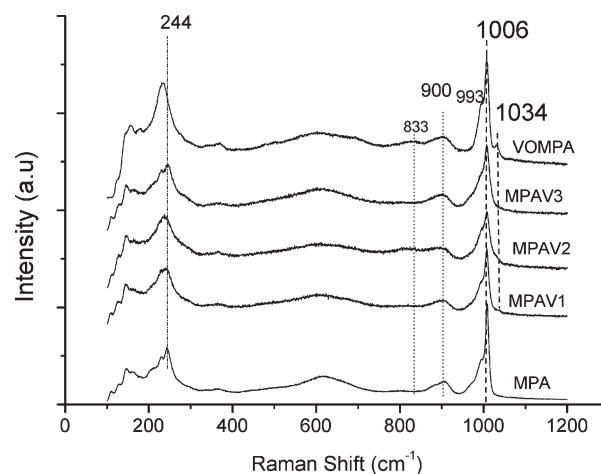
■ RESULTS

Solid-State ^{51}V MAS NMR Spectroscopy under Ambient Conditions. The solid-state ^{51}V MAS NMR spectra of the MPAV catalyst samples under ambient conditions are depicted
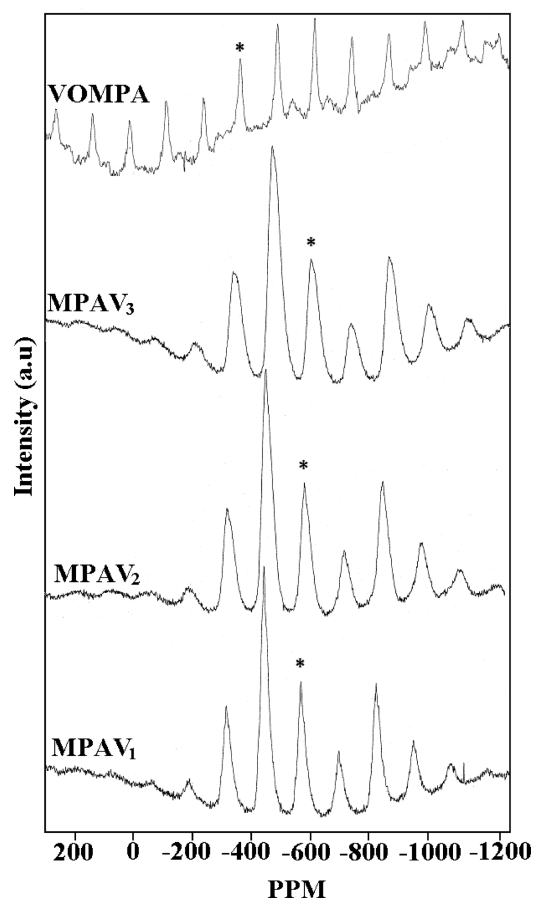
Figure 1. Solid-state ^{51}V MAS NMR spectra of the vanadium-containing POM catalysts. The notation (*) indicates the central NMR band.

Figure 2. In situ Raman spectra of dehydrated MPA, MPAV, and VOMPA POM catalysts at 200 °C.

in Figure 1. The MPAV1, MPAV2, MPAV3, and VOMPA catalysts possess central bands at −556, −556, −558, and −358 ppm, respectively. For reference, the ^{51}V MAS NMR spectrum of an ambient supported 20% V_2O_5/Al_2O_3 catalyst was also measured since this sample is known to consist of hydrated surface VO_6 units under ambient conditions that gives rise to a solid state ^{51}V MAS NMR band at −360 ppm.[23] This chemical shift matches that found for the VOMPA catalyst and indicates that VOMPA contains hydrated surface VO_6 units under ambient conditions that has previously been proposed to be a protonated $[O＝V(H_2O_5)_5]^{2+}$ complex.[9,24] The MPAV catalysts contain the primary solid state ^{51}V MAS NMR band at about −557 ppm indicating a different structure. The signal position at around −557 ppm has been assigned to octahedrally coordinated V^{5+} in the primary structure of the $H_4PMo_{11}VO_{40}$ Keggin ion.[9,24] The solid-state ^{51}V MAS NMR measurements, thus, confirm the different structures and locations of the dominant VO_x sites in the MPAV and VOMPA catalysts.

Infrared and Raman Spectroscopy under Ambient Conditions. The IR vibrations of the ambient Keggin POMs contain information about their structures, and the FT-IR spectra of the vanadium-containing MPAs and the V-free MPA are presented in the Supporting Information (Figure SF-1). Under ambient conditions, the Keggin samples are in a hydrated state containing waters of hydration.[24,25] The V-free MPA catalyst sample exhibits FT-IR bands at 1075 and 1003 cm^{-1} that have been assigned to the characteristic Keggin unit asymmetric stretching vibrations

of $\nu_{as}(P-O_a)$ and $\nu_s(Mo＝O_t)$, respectively.[26−28] The notations O_t, O_a, O_b, and O_c denote a terminal oxygen (Mo＝O), an oxygen atom bound to three Mo atoms and to one P atom (Mo_3-O_a-P), a corner sharing bridging oxygen atom ($Mo-O_b-Mo$), and an edge sharing bridging oxygen atom ($Mo-O_c-Mo$), respectively. The corresponding Raman vibrations provide complementary molecular structural information to that of FT-IR spectroscopy. The Raman spectrum of the V-free MPA POM under ambient conditions exhibits the characteristic bands of the MPA Keggin structure and is presented in the Supporting Information Figure SF-2 labeled RT with bands at 996 (s), 983 (w), 885 (w), 600 (w) and 248 (m) cm^{-1}. Adjacent Mo＝O_t bonds result in their vibrational coupling that give rise to ν_s and ν_{as} stretches with the symmetric mode being stronger in the Raman spectrum and the asymmetric mode stronger in IR spectrum.[29] The splitting of the Mo＝O_t vibration with ν_s (R-996 cm^{-1}) and ν_{as} (IR-1003 cm^{-1}) reflects the vibrational coupling of adjacent mono-oxo Mo＝O_t bonds in the MPA Keggin. The weak and broad bands at ∼885 and ∼600 cm^{-1} arise from the asymmetric $Mo-O_b-Mo$ and symmetric $Mo-O_c-Mo$ stretching modes, respectively. The strong band at 248 cm^{-1} corresponds to the bridging $Mo-O-Mo$ bending modes of the intact Keggin. Similar Raman spectra have been reported for unsupported MPA and MPAV samples under ambient conditions.[9,15,28,30] The Raman spectra of the ambient MPAV and VOMPA Keggins (see Supporting Information Figures SF-3 to SF-6 labeled RT) are partially dehydrated from laser induced dehydration because of the presence of the darker vanadium component in these POMs that also contribute to slightly blue shift the Raman bands to higher wavenumber.[31] The VOMPA Keggin also exhibits a distinct Raman band at 1034 cm^{-1} because of the presence of surface VO_x species on the outer surface of the MPA Keggin (see Supporting Information Figure SF-6).[29−31]

In Situ FT-IR and Raman Spectroscopy under Dehydrated Conditions. The in situ FT-IR spectra of the dehydrated MPA, MPAV, and VOMPA Keggins at 100 °C are presented in Figure SF-7 (see Supporting Information). Upon dehydration, the FT-IR bands for $\nu_{as}(P-O_a)$ and $\nu_{as}(Mo＝O_t)$ undergo a blue shift from 1075→1078 and 1003−10→1014 cm^{-1}, respectively.[26,27] The introduction of vanadium oxide onto the secondary surface of the POM Keggin structures is reflected by the presence of the
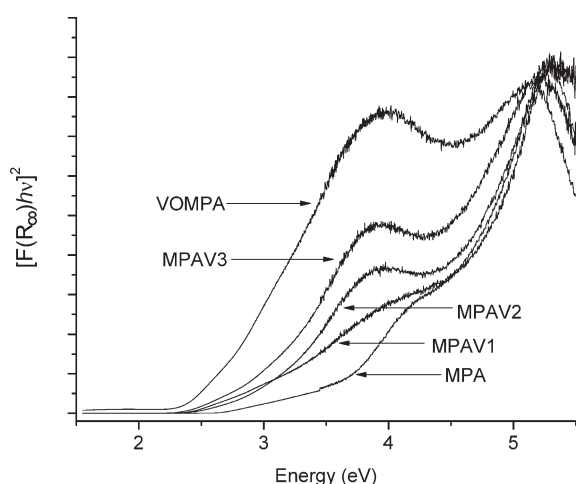
Figure 3. Normalized UV−vis Kubelka−Munk function spectra as a function of Incident Photon Energy (eV) for MPA, MPAV, and VOMPA POMs under ambient conditions.

small V═O band at ∼1034 cm^{-1}. The complementary in situ Raman spectra of the dehydrated MPA, MPAV, and VOMPA POM catalyst samples at 200 °C are presented in Figure 2. The Raman bands of the MPA and MPAV Keggins undergo a blue shift in the Mo═O$_t$ band from 996 to 1006 cm^{-1} upon dehydration at 200 °C. The blue shifts of the FT-IR and Raman bands are related to an increase in the M═O$_t$ bond order because of desorption of moisture.[32,33] The VOMPA sample exhibits the sharp MPA Keggin Raman bands and contains two new weak bands at ∼840 and 1034 cm^{-1} corresponding to an asymmetric Mo−O−V mode and a symmetric V═O$_t$ vibration of the dehydrated surface VO$_x$ species present in the secondary structure of Keggin ion, respectively.[34,35] Introduction of vanadium into the MPAV catalysts primarily results in broadening of the Raman bands of the MPA Keggin primary structure and the appearance of only a trace of the vanadyl V═O$_t$ band at 1034 cm^{-1}. The splitting of the M═O$_t$ vibration with v_{as}(IR-1014 cm^{-1}) and v_s(R-1006 cm^{-1}) reflect the vibrational coupling of adjacent Mo═O$_t$ bonds in the dehydrated Keggins. The terminal V═O$_t$ vibration appears at 1034 cm^{-1} in both the FT-IR and the Raman spectra, which indicates that this bond is not vibrationally coupled to adjacent Mo═O$_t$ bonds and is present as a mono-oxo functionality.[25]

Significant structural transformations of the MPA POMs take place at elevated temperatures since the Keggin structures begin to decompose (see Figures SF-2 to SF-6 in the Supporting Information). The V-free MPA Keggin structure destabilizes at 400 °C and forms β−MoO$_3$ crystals with characteristic new Raman bands at 850 and 775 cm^{-1}.[36] Upon further increasing the temperature to 500−600 °C, the crystalline β−MoO$_3$ phase transforms to the more thermally stable crystalline α−MoO$_3$ phase (Raman bands at 993, 818, 620, and 280 cm^{-1}). The thermal stability of the MPAV Keggins further decreases as more vanadium is introduced. The onset of β−MoO$_3$ formation for MPAV1 and VOMPA is still 400 °C, but decreases to 300 °C for MPAV2 and MPAV3. All the MPA Keggin catalysts, however, are thermally stable below 300 °C.

UV−vis Diffuse Reflectance Spectroscopy (DRS). The UV−vis DRS spectra of MPA, MPAV, and VOMPA catalyst samples were evaluated using the Kubelka−Munk function using the method of Davis and Mott[18] as further described by

Table 1. UV-vis DRS Edge Energy Values (eV) for MPA, MPAV, and VOMPA Catalysts under Ambient Conditions

catalyst	edge energy (eV) at ambient conditions
MPA	2.7 ± 0.1 eV
VOMPA	2.4 ± 0.1 eV
MPAV1	2.5 ± 0.1 eV
MPAV2	2.4 ± 0.1 eV
MPAV3	2.4 ± 0.1 eV

Gao[19] and Tian,[20] and the ambient spectra are shown in Figure 3. A broad, weak band occurs in MPA between 2.7 (460) and 3.7 (336) eV (nm), which corresponds to the leading linear region between 2.7 and 3.7 eV. The addition of vanadium to the MPA Keggin causes a broad band to appear between 2.4 (517 nm) and 3.9 eV (319 nm) which overlaps the first band of V-free MPA Keggin. The proximity of the molybdenum and vanadium UV−vis bands makes it difficult to obtain the desired electronic information for the individual molybdenum oxide and vanadium oxide components. The Eg values for each Keggin at ambient conditions are presented in Table 1 and reveal that the introduction of vanadium into both the primary and secondary structures lowers the Eg values. Note that the Eg values for the VOMPA and MPAV are almost the same indicating the insensitivity of UV−vis spectroscopy toward the specific location of the VO$_x$ in the MPA Keggin structure. Essentially the same UV−vis Eg values were also found for the ambient and dehydrated V-containing Keggins at room temperature indicating the invariance of Eg with the presence or absence of moisture.

In Situ FT-IR Spectroscopy of Chemisorbed CH$_3$OH. The in situ FT-IR spectra before and after methanol chemisorption at 100 °C on MPAV1 are presented in Supporting Information, Figure SF-8, in the 600−4000 cm^{-1} range. The vibrations at ∼1987 and ∼2127 cm^{-1} are the overtone bands of the Mo═O$_t$ and P═O$_a$ vibrations, respectively, and the broad band at ∼3280 cm^{-1} is associated with the delocalized H$^+$ protons of the MPA Keggin. The difference FT-IR spectrum does not reveal any strong vibrations from the chemisorbed or physisorbed methanol (C−H vibrations at 2800−3000 cm^{-1}) because of the low Keggin surface area and, consequently, the low number of adsorbed methanol molecules. By comparison with previous studies on methanol sorption by tungstophosphoric acid (TPA), it is anticipated that less than 1 CH$_3$OH/H$^+$ exists after methanol adsorption at 100 °C.[37]

CH$_3$OH-TPSR Spectroscopy. The surface chemistry of the MPA, MPAV, and VOMPA Keggin catalyst systems was chemically probed with CH$_3$OH-TPSR spectroscopy since the surface reaction pathways of the methanol derived surface intermediates are well-known: dehydrogenation of surface CH$_3$O* to form H$_2$CO on surface redox sites and deoxygenation of surface CH$_3$O* on surface acid sites with the resulting *CH$_3$ fragment reacting with adjacent surface CH$_3$O* to form CH$_3$OCH$_3$ (DME).[38] The CH$_3$OH-TPSR experiments with the vanadium-containing MPA catalyst samples yield formaldehyde as the main reaction product with only minor formation of DME. The HCHO/CH$_3$OH-TPSR spectra are presented in Figure 4(a−e) and the DME/CH$_3$OH spectra are not shown for brevity because of their very weak signals. The vanadium-free MPA catalyst exhibits the major HCHO formation with a Tp of 220 °C and a weaker amount of HCHO formed at ∼412 °C. As the vanadium is introduced into the MPA Keggin, the major
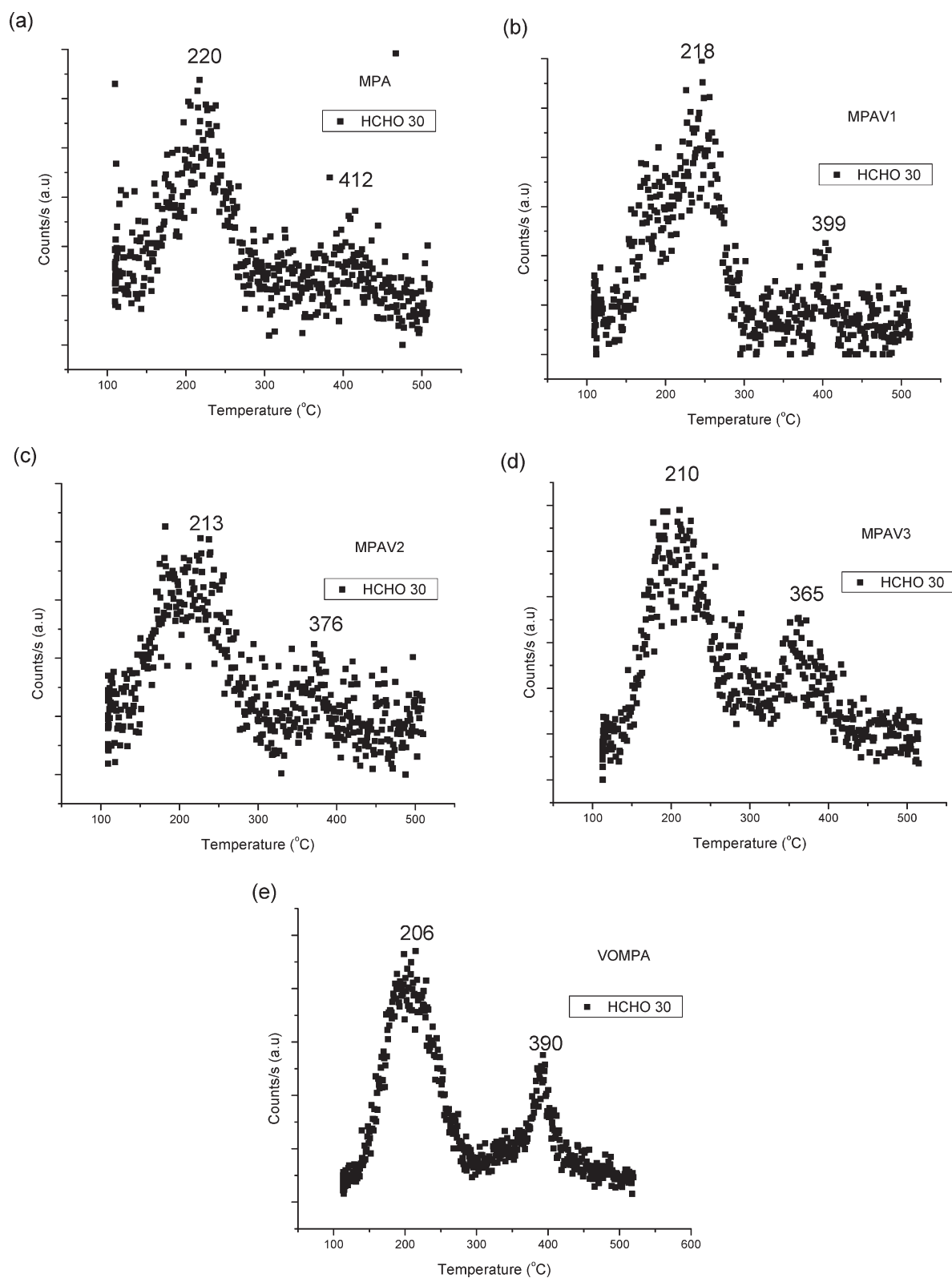
Figure 4. CH$_3$OH-TPSR spectra from (a) MPA, (b) MPAV1, (c) MPAV2, (d) MPAV3, and (e) VOMPA POM catalysts.

HCHO Tp temperature slightly decreases from 220 to 210 °C for the MPAV catalysts and occurs at 206 °C for the VOMPA catalyst. The presence of the smaller HCHO peak in the 350−450 °C range suggests a minor secondary site for the

chemisorbed CH$_3$OH species that increases with VO$_x$ content in the MPAV Keggin and exhibits the strongest contribution for the VOMPA Keggin catalyst. The Tp value of the secondary HCHO monotonically decreases with increasing vanadium content
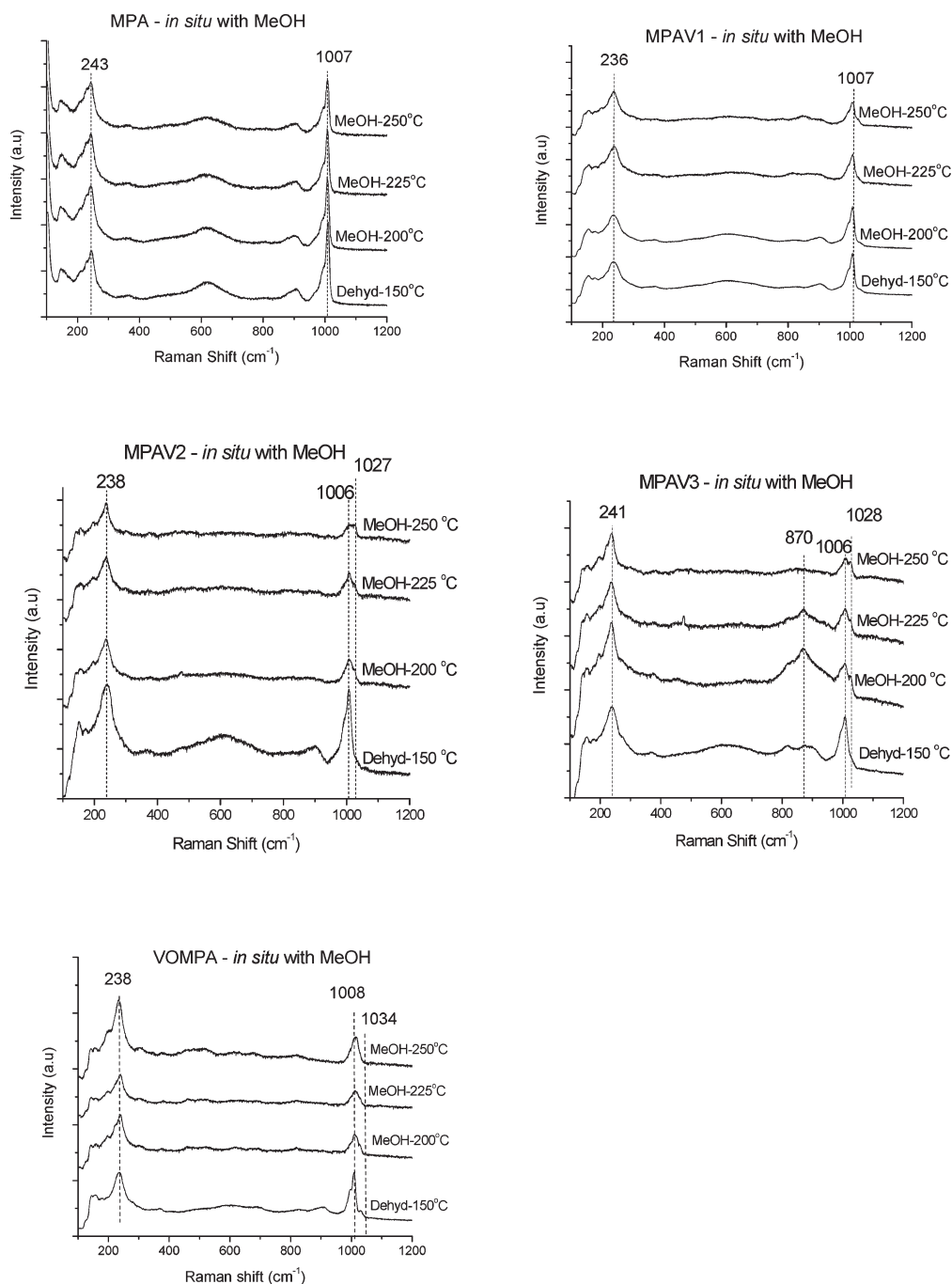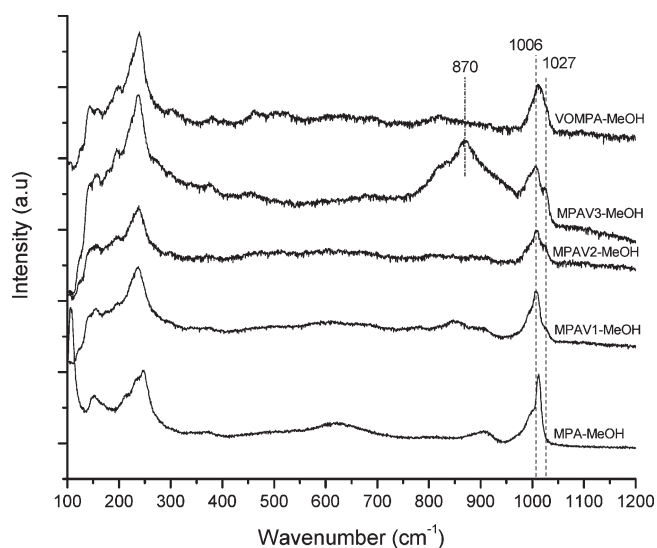
Figure 5. In situ Raman spectra of MPA, MPAV, and VOMPA POM catalysts during methanol oxidation/dehydration between 150 and 250 °C in flowing $CH_3OH/O_2/He$.

in MPAV: MPA (412 °C), MPAV1 (399 °C), MPAV2 (376 °C), and MPAV3 (365 °C). The VOMPA Keggin exhibits the secondary HCHO Tp value of 390 °C. Interestingly, the production of the secondary HCHO corresponds to the range where the Keggins decompose and also coincide with the individual Keggin decomposition temperatures (see SF-2 to SF-6 in Supporting Information).

In Situ Raman Spectroscopy during CH_3OH Oxidation/ Dehydration. The in situ Raman spectra of the MPA, MPAV, and VOMPA POM catalysts during methanol oxidation/dehydration between 150 and 250 °C were collected to better

understand the bulk and surface structural changes during steady-state methanol oxidation/dehydration reaction conditions and are shown in Figure 5. None of these catalysts formed any coke deposits (Raman bands at ~1400 and ~1600 cm^{-1}) during methanol oxidation, which reflects the efficient redox nature of these POMs. The V-free MPA Keggin catalyst retains its ordered structure during methanol oxidation/dehydration as reflected by its sharp $Mo=O_t$ Raman band at 1007 cm^{-1} over the temperature range 200–250 °C. The Raman bands for the MPAV catalysts, however, are much broader, which reflects the structural disorder of the MPAV Keggins, and they also exhibit a

Figure 6. In situ Raman spectra of MPA, MPAV, and VOMPA POM catalysts during methanol oxidation/dehydration at 225 °C with O_2/CH_3OH = 2.17.

shoulder at $\sim$1027 cm^{-1} from the $\nu(V{=}O_t)$ vibration of the expelled VO_x unit. The slight red shift of the V$=$O$_t$ Raman band position from 1034 to 1027 cm^{-1} is related to the presence of methanol surface reaction intermediates residing on the catalyst under reaction conditions.[38] The extent of broadening of the Keggin Raman bands and the amount of expelled VO_x increase with (*i*) vanadium oxide content, (*ii*) exposure to the methanol oxidation/dehydration reaction conditions, and (*iii*) reaction temperature. The in situ Raman spectra of the MPA, MPAV, and VOMPA Keggin catalysts under methanol oxidation at 225 °C are compared in greater detail in Figure 6 and confirm that the concentration of expelled surface VO_x species (weak band at $\sim$1027 cm^{-1}) under reaction conditions increases with vanadium content for the MPAV catalysts. For the MPAV3 catalyst, the Keggin structure begins to decompose to $\beta$$-MoO_3$ nanoparticles as reflected by the broad Raman bands at $\sim$870 and $\sim$814 cm^{-1}. In contrast, only a trace amount of expelled VO_x is present for the MPAV Keggins prior to exposure to the methanol oxidation/dehydration reaction conditions (see Figures 4 and Supporting Information SF-3 to SF-6). It, thus, appears that during methanol oxidation/dehydration reaction conditions the MPAV Keggin catalysts always possess some expelled surface VO_x species with the primary MPA Keggin structural units becoming disordered.

In Situ UV$-$vis Spectroscopy during CH$_3$OH Oxidation/Dehydration. Complementary oxidation state information about the Mo and V cations in the MPA, MPAV, and VOMPA Keggin catalysts during methanol oxidation was provided by in situ UV$-$vis spectroscopy, and the spectra are presented in Figures 7a$-$f. The Mo(VI) oxidation state in MPA Keggin exhibits a broad ligand to metal charge transfer (LMCT) band at approximately 430 nm as shown in Figure 7b, and the octahedral V(V) oxidation state gives rise to an overlapping broad LMCT band at $\sim$480 nm as seen in the bulk V_2O_5 reference compound (Figure 7a).[3,39] The in situ UV$-$vis spectra reveal that the Mo(VI) LMCTs for MPA, MPAV, and VOMPA are not diminished during methanol oxidation indicating that the Mo cations are still oxidized under the chosen reaction conditions. The same conclusion can also be made for the

V(V) cations, but it is apparent that a minor amount of the V(V) and Mo (VI) species become reduced during the chosen thermal treatment and methanol oxidation reaction conditions. Since UV$-$vis is particularly sensitive to coloration changes, a minor amount of reduction is easily detected. The quantitative analysis of the reduction of the V(V) cations with UV$-$vis spectroscopy is somewhat complicated because of the overlap of the strong Mo(VI) LMCT band with that of the V(V) LMCT band. Nevertheless, the V cations appear to be primarily oxidized under the net oxidizing methanol oxidation reaction conditions ($10\%O_2$/Ar 15 mL/min and 2000 ppm CH_3OH/He 15 mL/min).

Steady-State CH$_3$OH Oxidation/Dehydration. The steady-state methanol oxidation/dehydration results at 230 °C over these POM Keggin catalysts are listed in Table 2. Dimethyl ether (H_3COCH_3) and formaldehyde (HCHO) were the major reaction products, and methyl formate (H_3COOCH) and dimethoxymethane ($H_2C(OCH_3)_2$) were only minor reaction products under the present experimental conditions. The V-free MPA Keggin primarily yields DME, which reflects its acidic nature, but also produces a minor amount of HCHO indicating its limited redox character. Introduction of the VO_x sites into the MPA Keggin, however, increases the TOF_{redox} by a factor of $\sim$4$-$6 and the HCHO selectivity by a factor of $\sim$3$-$5. The highest HCHO selectivity is observed for the VOMPA catalyst where surface VO_x species exclusively replace the acidic H$^+$ sites in the secondary Keggin structure. The TOF_{redox} values for the MPAV Keggins are dominated by the VO_x sites, and the values decrease with vanadium oxide content. Although the highest HCHO selectivity is observed for the VOMPA catalysts, the VOMPA TOF_{redox} value is comparable to that of the MPAV2 catalyst.

■ DISCUSSION

Bulk or Primary Keggin Structures. The ambient H_{3+x}PMo$_{12-x}$V$_x$O$_{40}$ Keggins retain their primary MPA structure upon incorporation of vanadium oxide (see Figures 2$-$4 and Supporting Information section for SF-2 to SF-6). Incorporation of vanadium oxide into the MPA Keggin primary structure is confirmed with solid-state ^{51}V MAS NMR (shown in Figure 1). Incorporation of VO_x sites into the MPA Keggin structure also lead to broadening of the vibrational bands of the primary Keggin structure (shown in Supporting Information, Figures SF-2 to SF-6) reflecting the structural disorder caused by incorporation of VO_x units into MPA. The extent of structural disorder in the MPAV Keggins increases with the number of incorporated VO_x units. Despite this structural disorder, the Keggin structure is retained under ambient conditions. The UV$-$vis Eg value of the MPA Keggin is only slightly decreased by $\sim$0.2$-$0.3 eV by the introduction of the VO_x units into the MPA Keggin structure and, surprisingly, is independent of the number of inserted VO_x units. The slightly lower Eg values of the MPAV Keggins correspond to the slightly greater electron delocalization introduced by the addition of vanadium oxide. When the Eg values for MPAV are evaluated using the V$-$O$-$V correlation published by Gao et al.,[19] the correlation indicates that four bridging V$-$O$-$V bonds are present for every V-containing MPA Keggin. The V-containing MPA Keggins, however, mostly contain V$-$O$-$Mo and not V$-$O$-$V bonds because of the minority concentration of vanadium oxide. Therefore, this indicates that the correlation developed by Gao et al.[19] is also applicable when the vanadium cation is bridge bonded to other cations such as Mo.
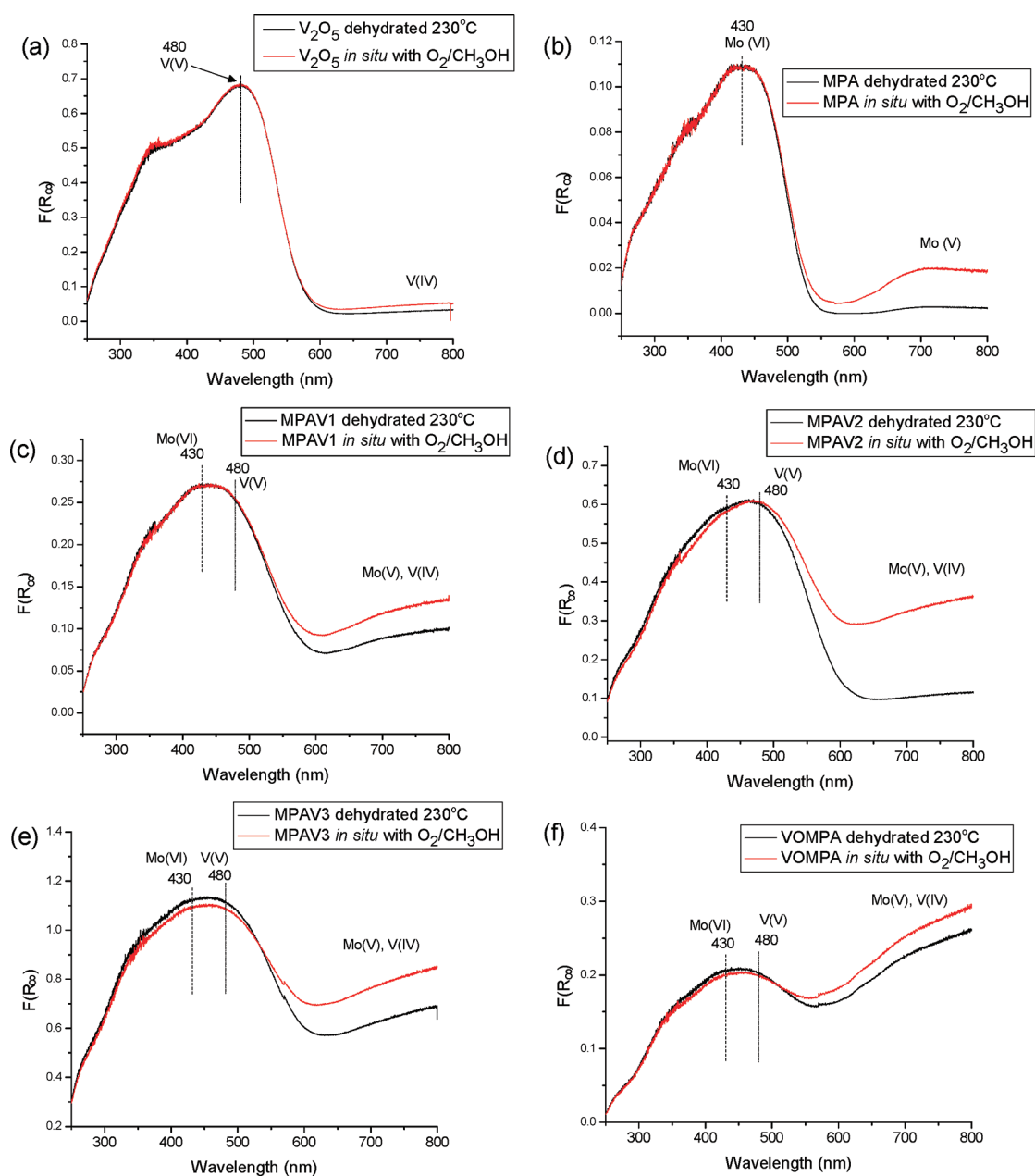
Figure 7. In situ UV−vis Kubelka−Munk spectra of (a) Bulk V_2O_5 reference compound, (b) MPA, (c) MPAV1, (d) MPAV2, (e) MPAV3, and (f) VOMPA POMs upon dehydration at 230 °C and during methanol oxidation/dehydration at 230 °C with $O_2/CH_3OH = 2.17$.

Dehydration of the MPAV Keggins results in the removal of the crystal water and shifts the $\nu_s(Mo{=}O_t)$ from ∼996 to ∼1006−1009 cm^{-1} (see Figures SF-3 to SF-6 in Supporting Information). The introduction of VO$_x$ introduces structural disorder of the MPAV Keggins (see Figures 2 and Supporting Information section for Figures SF-2 to SF-6) that is enhanced with increasing sample temperature. The MPAV Keggin structural disorder facilitates the decomposition of the $H_{3+x}PMo_{12-x}V_xO_{40}$ Keggin primary structure to crystalline $\beta-MoO_3$ nanoparticles at 300 °C and above, which transform to the thermodynamically stable crystalline $\alpha-MoO_3$ phase at 500−600 °C. MPA, MPAV1, and MPAV2 remain as intact Keggins upon dehydration as evidenced by the lack of decomposition bands as described by Mestl et al. in the "terminal stretching regime".[15] The lower thermal stability of the MPAV Keggins with increasing vanadium

content is related to the lower Tammann temperature of vanadium oxide (V_2O_5) compared to that of molybdenum oxide (MoO_3), ∼200 vs. ∼300 °C, respectively. The lower Tammann temperature of vanadium oxide enhances its mobility and, thus, leads to easier vanadium oxide expulsion from the Keggin primary structure to its surface secondary structure with subsequent decomposition of the MPA into its metal oxide constituents. The supported VOMPA Keggin catalyst, where VO$_x$ is introduced onto the secondary Keggin structure, possesses greater structural order and thermal stability than the MPAV catalysts possessing VO$_x$ in the primary Keggin structure (see Figures SF-2 to SF-6 in Supporting Information section). Thus, the extent of disorder and thermal stability of the primary MPA Keggin structure is mostly influenced by the VO$_x$ incorporated into the Keggin primary structure rather than the presence of surface VO$_x$ units.

Table 2. Steady-State Methanol Oxidation/Dehydration Data for MPA, MPAV, and VOMPA Catalysts[a]

| catalysts | temp. (°C) | conv. (%) | activity (mol/g. cat·s) | selectivity (%) | | | | TOF_{redox} (s^{-1}) |
				DME	HCHO	MF	DMM	
MPA	230	5.7	3.0	93	7			0.018[b]
MPAV1	230	12.0	6.4	72	24	3	1	1.8
MPAV2	230	15.0	8.0	67	31	1	1	1.3
MPAV3	230	12.7	6.8	76	23		1	0.52
VOMPA	230	8.1	4.3	60	34	3	3	1.1

[a] $CH_3OH/O_2/He = 6/13/81$ and 100 mL/min. [b] Molybdenum redox activity only. For V-containing catalysts, vanadium redox activity only since minor Mo redox contribution has been subtracted.

Although the MPA and MPAV Keggin primary structures are thermally stable below 300 °C, the MPAV catalysts undergo further bulk structural changes upon exposure to the methanol oxidation/dehydration reaction conditions (see Figures 5 and 6). The Raman bands of the primary Keggin structure of the MPAV catalysts further broaden and some poorly ordered $\beta-MoO_3$ nanoparticles are also present for MPAV3. The partial transformation of MPAV3 to $\beta-MoO_3$ during methanol oxidation/dehydration is probably related to the formation of mobile surface $Mo-OCH_3$ complexes in the reactive methanol environment.[40] The appearance of expelled VO_x units, Raman band at $\sim$1027 cm^{-1}, indicates that the VO_x units originally incorporated into the $H_{3+x}PMo_{12-x}V_xO_{40}$ Keggin primary structure are being expelled in the corrosive methanol environment. The expulsion of the VO_x units from the MPAV Keggin primary structure is most likely also related to the formation of mobile surface VO_x and $V-OCH_3$ complexes in the reactive methanol environment. The expulsion of VO_x units from MPAV bulk structure was previously also reported for isobutane oxidation, which suggests that this is a general phenomenon for MPAV Keggin catalysts under oxidation reaction conditions at elevated temperatures.[7]

Surface or Secondary Keggin Structures. The selective introduction of VO_x units onto the secondary MPA Keggin structure for the supported VOMPA Keggin was confirmed with solid-state ^{51}V MAS NMR (see Figure 1) and the lack of perturbation of the primary MPA Keggin vibrations as detected by Raman spectroscopy (see Figure 2). In situ Raman studies of the dehydrated VOMPA catalyst confirm that the introduced VO_x species are present in the MPA Keggin secondary structure as dehydrated surface VO_x species (Raman band at $\sim$1034 cm^{-1} under dehydrated conditions). The UV–vis Eg value for the surface VO_x species is indistinguishable from that of the VO_x unit incorporated into the primary MPAV Keggin structure. Unlike the supported VOTPA (TPA: tungstophosphoric acid) catalyst where there is coupling between the $V=O_t$ and $W=O_t$ vibrations,[39] vibrational coupling between $V=O_t$ and $Mo=O_t$ does not appear to occur for the supported VOMPA system since the $V=O_t$ and $Mo=O_t$ Raman bands always occur at $\sim$1034 and $\sim$1007 cm^{-1}, respectively. One possible reason is that the $Mo=O_t$ vibration (1007 cm^{-1}) occurs at a lower value than the $W=O_t$ vibration (1022 cm^{-1}), with the latter being closer to the $V=O_t$ vibration (1034 cm^{-1}). Although only a small amount of surface VO_x species are initially present in the secondary structures of the MPAV catalysts, the quantity of surface VO_x species further increases upon exposure to the reactive methanol oxidation/dehydration reaction. The occurrence of the $V=O_t$

vibration at $\sim$1027–1034 cm^{-1} coincides with the vibration of mono-oxo surface $O=V(-O-Support)_3$ species present on oxide supports. Thus, the structure of the surface vanadium species present in the MPA Keggin secondary structure is tentatively assigned as $O=V(-O-Mo)_3$.[20,31,36]

Surface Chemistry. The primary reaction product from CH_3OH-TPSR over the MPA, MPAV, and VOMPA Keggin catalysts is HCHO from redox sites, 206 °C < Tp < 220 °C, with surprisingly small amounts of DME formed from the acidic sites under these experimental conditions. Although the chemisorbed methanol species escaped direct IR detection because of the low catalyst surface area, redox sites will convert both surface intact CH_3OH^* and CH_3O^* to HCHO.[38] The slight decrease in the HCHO formation Tp value upon the introduction of VO_x in the MPAV Keggins indicates that redox VO_x sites are slightly more active than MoO_x sites for conversion of the surface methanol intermediates to HCHO. The HCHO/CH_3OH-TPSR Tp temperatures for the MoO_x sites and the VO_x sites in the MPA and MPAV Keggins exhibit comparable Tp values to those previously reported for bulk MoO_3,[41−43] supported MoO_3,[41−43] bulk mixed metal molybdates,[43] bulk V_2O_5,[41−43] supported V_2O_5,[42−44] and bulk mixed metal vanadate catalysts.[43] The appearance of the secondary HCHO formation peak with such high temperatures of 365 °C < Tp < 412 °C has not previously been reported during CH_3OH-TPSR spectroscopy experiments with molybdates and vanadates.[37−40] As already mentioned, this temperature region and even the Tp trend corresponds to the temperatures where the MPA and MPAV Keggin structures decompose (see Figures SF-2 to SF-6 in Supporting Information). It, thus, seems that the second burst of HCHO formation must originate from CH_3OH^* or possibly CH_3O^* species dissolved within the bulk MPA Keggin structure. The sorption of CH_3OH by POM Keggins at modest temperatures ($T < 250$ °C) is well documented in the literature.[11,37,45−47] The sorbed methanol has been proposed to be present in the Keggins as protonated $(CH_3OH)_nH^+$ clusters with n varying from 1 to 4 at low temperatures ($T < 150$ °C) and completely desorbed by 250 °C based on TGA measurements.[37] The prior TGA studies only examined the temperature range of 25–300 °C where the Keggin structure was still intact. It should be noted that these studies chemisorbed methanol at 25–50 °C where physically adsorbed methanol forms[11] and that in the present investigation chemisorption was purposely performed at 100 °C to minimize the low temperature physisorbed methanol.[20]

The current CH_3OH-TPSR findings that HCHO is still being formed at much higher temperatures of 350–450 °C reveal for the first time that residual sorbed methanol is still present *within* the Keggin POM structures until the Keggin structures

decompose and simultaneously lead to reaction with the sorbed methanol.

The ability to perform the HCHO/CH$_3$OH-TPSR experiments in the absence of gas phase molecular O$_2$, in flowing He, further demonstrates that methanol oxidation to formaldehyde reaction by MPA, MPAV, and VOMPA proceeds via the Mars-van Krevelen reaction mechanism that is consistent with steady-state zero-order kinetics in O$_2$ partial pressure previously reported for oxidation reactions by MPAV Keggin catalysts.[6] This is further reflected in the predominance of the V^{+5} oxidation state during methanol oxidation reaction conditions (see Figure 7).

Structure-Catalytic Activity Relationships. Three distinct redox sites are present in the MPA, MPAV, and VOMPA Keggin catalysts: MoO$_x$ in the primary Keggin structure, VO$_x$ in the primary Keggin structure, and surface VO$_x$ in the secondary Keggin structure. The MoO$_x$ sites in the primary MPA Keggin structure are significantly less reactive for redox chemistry, by a factor of $\sim$10^{-2}, than the VO$_x$ sites in the primary MPA Keggin structure and the surface VO$_x$ sites present in the Keggin secondary structure. The steady-state TOF$_{redox}$ values for the MPAV Keggins slightly decrease with vanadium oxide content, and this is ascribed to the MPA structural disorder that is resulting from incorporation of the vanadium oxide since the reactivity decrease parallels the increased structural disorder resulting from incorporation of VO$_x$ units into the MPA Keggin primary structure. It is also possible that the decrease is simply attributed to experimental error. Still, the decrease is not related to the presence of surface VO$_x$ site since VOMPA and MPAV2 have comparable TOF$_{redox}$ values and VOMPA does not exhibit structural disorder from the presence of surface VO$_x$ units on the MPA Keggin. However, it is important to recognize that MPAV3 is a unique case. The decrease by a factor of $\sim$3.5 in the TOF for MPAV3 is not solely because of increasing vanadium content, but is related to incipient Keggin decomposition to β−MoO$_3$. The decomposition of MPAV3 to β−MoO$_3$ is also illustrated in Figure 6 with the appearance of broad bands at $\sim$814 and 870 cm^{-1}. MPAV3 is more structurally disordered than MPAV1, MPAV2, or VOMPA and, therefore, is more prone to decomposition especially in the corrosive methanol environment. Previously, Sorenson and Weber proposed that CH$_3$OH oxidation to HCHO only requires one VO$_x$ site since they found that TOF$_{redox}$ was independent of VO$_x$ incorporation into their Na-MPA Keggins.[48] The present study finds a slight decrease in TOF$_{redox}$ with increasing vanadium oxide incorporation because of the absence of the stabilizing Na in the current MPAV Keggin catalysts. For only one participating VO$_x$ unit required for methanol oxidation, the TOF$_{redox}$ should be approximately constant with number of VO$_x$ units in the MPA Keggin primary structure, which is qualitatively observed and the slight decrease is associated with the corresponding increasing structural disorder. For CH$_3$OH oxidation to HCHO to require two adjacent VO$_x$ sites, then the TOF$_{redox}$ would be expected to increase by a factor of 9 in going from MPAV1 to MPAV3, which is not the case. The current findings of a relatively constant TOF$_{redox}$ with number of VO$_x$ units in the MPA Keggin (excluding the case of MPAV3, which has partially decomposed to β−MoO$_3$) are, thus, in agreement with the conclusions of Sorenson and Weber that methanol oxidation to formaldehyde only requires one VO$_x$ site.[45] These experimental conclusions are also supported by recent density functional theory (DFT) calculations showing that CH$_3$OH oxidation to HCHO readily proceeds on only one VO$_x$ unit.[46,47]

The steady-state TOF$_{redox}$ value for methanol oxidation by the V-free MPA Keggin is 0.018 s^{-1} and comparable to that for bulk MoO$_3$, $\sim$0.02−0.05 s^{-1}, at 230 °C.[41,49] The V-free MPA Keggin, however, is much more acidic than bulk MoO$_3$ yielding primarily DME whereas bulk MoO$_3$ primarily forms HCHO as the dominant methanol oxidation product. The CH$_3$OH equilibrium adsorption constant K_{ads} must be slightly greater for MPA than for bulk MoO$_3$ to compensate for the somewhat slower surface methoxy C−H bond breaking step (220 vs. 196 °C, respectively).

The steady-state TOF$_{redox}$ values for methanol oxidation over the H$_{3+x}$PMo$_{12-x}$V$_x$O$_{40}$ Keggins, $\sim$0.4 s^{-1}, are comparable to that for bulk V$_2$O$_5$, $\sim$0.2−1 s^{-1}, at 230 °C.[41,42,49] The TOF$_{redox}$ for VOMPA, 0.13 s^{-1}, is also comparable to the more active supported vanadium oxide catalysts such as supported V$_2$O$_5$/TiO$_2$ (0.11 s^{-1}) and V$_2$O$_5$/ZrO$_2$ (0.17 s^{-1}) at 230 °C. Where bulk and supported vanadium oxide catalysts almost exclusively yield HCHO as the reaction product, the Keggin catalysts give DME as a major reaction product. This difference reflects the much stronger acidic character of the Keggin-type catalysts. The CH$_3$OH K_{ads} must also be slightly greater on the Keggin catalysts than the non-Keggin catalysts since the Keggin catalysts exhibit CH$_3$OH-TPSR Tp values for surface methoxy C−H bond breaking of 210−220 °C and the non-Keggin vanadia catalysts show Tp values of 180−190 °C.[41,42,49,50] Thus, the redox character of VO$_x$ and MoO$_x$ sites in the Keggins exhibit comparable steady-state methanol oxidation TOF$_{redox}$ values as found for bulk MoO$_3$, bulk V$_2$O$_5$, and supported vanadium oxide catalysts, but the highly acidic nature of the Keggins affects their catalytic performance.

The enhanced redox catalytic activity of the V-containing Keggins relative to H$_3$PMo$_{12}$O$_{40}$ is also in agreement with the slightly lower Eg values of the H$_{3+x}$PMo$_{12-x}$V$_x$O$_{40}$ Keggins (see Table 1) and the higher specific catalytic reaction rates of vanadium oxides relative to molybdenum oxides.[50] There is no relationship, however, between the Keggin UV−vis Eg values and the number of VO$_x$ sites in the H$_{3+x}$PMo$_{12-x}$V$_x$O$_{40}$ Keggin (all the Eg values are comparable at 2.4−2.5 $\pm$ 0.1 eV) as well as independent of the location of the VO$_x$ site in the H$_{3+x}$PMo$_{12-x}$V$_x$O$_{40}$ Keggin (primary structure exhibits Eg at 2.4−2.5 $\pm$ 0.1 eV and secondary structure at 2.4 $\pm$ 0.1 eV).

As already discussed above, the oxidation of methanol to formaldehyde over the MPAV Keggin catalysts proceeds via a Mars-van Krevelen mechanism that exhibits zero-order dependence on the oxygen partial pressure. The methanol oxidation reaction over the MPAV Keggins, however, exhibits a slight positive dependence on the methanol partial pressure as previously found by Liu and Iglesia.[6] The weak dependence of the reaction rate on the methanol partial pressure suggests that the methanol sorbed within the Keggin structure is not able to sufficiently provide methanol or methoxy species toward HCHO formation. The sorbed methanol within the Keggin is not able to rapidly provide sufficient reactive methanol or methoxy species since the reaction dependence on methanol partial pressure is not exactly zero-order as found for the rapid supply of oxygen from the Keggin lattice.

Pretreatment and reaction temperatures of the Keggin catalysts have been found to affect both methanol conversion rate and product selectivity during methanol oxidation by the MPAV Keggins.[6] Increasing the thermal pretreatment temperature decreases the conversion of methanol and was attributed to the loss of surface Bronsted acid sites. The new findings in the present investigation suggest that the situation is actually more

complex involving both changes in surface Bronsted acidity and surface composition. As the pretreatment temperature is increased, the VO_x sites in the primary Keggin structure are expelled from the lattice onto the Keggin external surface or secondary structure (see Figures SF-3 to SF-6 in Supporting Information). This leads to two simultaneous consequences: (1) the expelled surface VO_x sites anchor on the exterior Keggin surface by consuming the surface Bronsted acid hydroxyls and (2) convert the somewhat more active VO_x sites originally in the Keggin primary structure to slightly less reactive surface VO_x sites on the Keggin external surface. The first consequence suppresses the surface Bronsted acidity relative to the surface redox properties, which shifts the reaction selectivity toward redox products relative to acidic products with increasing temperature. The second consequence decreases the overall catalyst activity as somewhat more active VO_x sites in the Keggin primary structure are converted to slightly less active surface VO_x sites on the Keggin external surface (secondary structure). Thus, it is the simultaneous decrease in surface Bronsted acidity and VO_x reactivity that influences the overall catalytic performance of the MPAV Keggin catalysts.

CONCLUSIONS

Incorporation of VO_x units into the primary $H_{3+x}PMo_{12-x}V_xO_{40}$ Keggin structure by substitution for MoO_x sites leads to (*i*) disorder of the primary Keggin structure, (*ii*) decrease in thermal stability of the Keggin, (*iii*) preferential expulsion of the VO_x units from the primary structure into the secondary structure under reaction conditions and elevated temperatures, and (*iv*) transformation of the Keggin to crystalline MoO_3 phases at elevated temperatures. The dynamic nature of the POM Keggins underscores the importance of performing in situ characterization studies under relevant reaction conditions. Consequently, caution should be maintained when treating POM Keggins as static ideal model structures, especially at reaction conditions that take place at elevated temperatures ($T > 100\ °C$).

The relative reactivity of the MoO_x and VO_x cations in the $H_{3+x}PMo_{12-x}V_xO_{40}$ Keggin structure for methanol oxidation to formaldehyde is $VO_{x,primary} > VO_{x,secondary} \gg MoO_{x,\ primary}$. This reactivity trend is related to the greater electron delocalization introduced by incorporation of the VO_x units as reflected in the lower UV−vis Eg values, but there is no correlation between the UV−vis Eg values and the steady-state TOF_{redox}. The greater reactivity of the VO_x sites relative to the MoO_x sites allows for determining the influence of the number of VO_x sites upon the methanol oxidation reaction. The relative independence of the TOF_{redox} values as a function of the number of VO_x sites in the MPAV Keggin is in agreement with the Sorenson and Weber conclusion that only one VO_x site is required for methanol oxidation to formaldehyde reaction[41] and is consistent with recent DFT calculations.[46,47]

ASSOCIATED CONTENT

S **Supporting Information.** Additional ambient, dehydrated, and in situ FT-IR spectra, and in situ Raman spectra of the V-containing Keggins as a function of calcination temperature. This material is available free of charge via the Internet at http://pubs.acs.org.

AUTHOR INFORMATION

Corresponding Author
*Phone: +1 610 758 4274. Fax: +1 610 758 5057. E-mail: iew0@lehigh.edu.

Present Addresses
†Catalysis Laboratory, I&PC Division, Indian Institute of Chemical Technology, Hyderabad, India 500 607.
‡Chemical Sciences and Engineering Division, Argonne National Laboratory, Argonne, IL 60439.

REFERENCES

(1) Okuhara, T.; Mizuno, N.; Misono, M. In *Advances in Catalysis*; Eley, D. D.; Haag, W. O.; Gates, B., Eds.; Academic Press: London, 1996; Vol. 41, p 113.

(2) Cavani, F.; Mezzogori, R.; Pigamo, A.; Trifirò, F.; Etienne, E. *Catal. Today* **2001**, *71*, 97–110.

(3) Melsheimer, J.; Mahmoud, S. S.; Mestl, G.; Schlögl, R. *Catal. Lett.* **1999**, *60*, 103–111.

(4) Bruckman, K.; Tatibouet, J. M.; Che, M.; Serwicka, E.; Haber, J. *J. Catal.* **1993**, *139*, 455–467.

(5) Liu, H.; Iglesia, E. *J. Catal.* **2004**, *223*, 161–169.

(6) Liu, H.; Iglesia, E. *J. Phys. Chem. B* **2003**, *107*, 10840–10847.

(7) Watzenberger, O.; Emig, G.; Lynch, D. T. *J. Catal.* **1990**, *124*, 247–258.

(8) Brückner, A.; Scholz, G.; Heidemann, D.; Schneider, M.; Herein, D.; Bentrup, U.; Kant, M. *J. Catal.* **2007**, *245*, 369–380.

(9) Blouet-Crusson, E.; Rigole, M.; Fournier, M.; Aboukaïs, A.; Daubrege, F.; Hecquet, G.; Guelton, M. *Appl. Catal., A* **1999**, *178*, 69–83.

(10) Ilkenhans, T.; Herzog, B.; Braun, T.; Schlogl, R. *J. Catal.* **1995**, *153*, 275–292.

(11) Fournier, M.; Louis, C.; Che, M.; Chaquin, P.; Masure, D. *J. Catal.* **1989**, *119*, 400–414.

(12) Lee, J. K.; Melsheimer, J.; Berndt, S.; Mestl, G.; Schlögl, R.; Köhler, K. *Appl. Catal., A* **2001**, *214*, 125–148.

(13) Ressler, T.; Timpe, O.; Girgsdies, F.; Wienold, J.; Neisius, T. *J. Catal.* **2005**, *231*, 279–291.

(14) Nair, H.; Miller, J. T.; Stach, E. A.; Baertsch, C. D. *J. Catal.* **2010**, *270*, 40–47.

(15) Mestl, G.; Ilkenhans, T.; Spielbauer, D.; Dieterle, M.; Timpe, O.; Kröhnert, J.; Jentoft, F.; Knözinger, H.; Schlögl, R. *Appl. Catal., A* **2001**, *210*, 13–34.

(16) Lee, J. K.; Russo, V.; Melsheimer, J.; Köhler, K.; Schlögl, R. *Phys. Chem. Chem. Phys.* **2000**, *2*, 2977–2983.

(17) Casarini, D.; Centi, G.; Jiru, P.; Lena, V.; Tvaruzkova, Z. *J. Catal.* **1993**, *143*, 325–344.

(18) Davis, E. A.; Mott, N. F. *Philos. Mag.* **1970**, *22*, 903–922.

(19) Gao, X.; Wachs, I. E. *J. Phys. Chem. B* **2000**, *104*, 1261–1268.

(20) Tian, H.; Roberts, C. A.; Wachs, I. E. *J. Phys. Chem. C* **2010**, *114*, 14110–14120.

(21) Feng, T.; Vohs, J. M. *J. Catal.* **2002**, *208*, 301–309.

(22) Briand, L. E.; Farneth, W. E.; Wachs, I. E. *Catal. Today* **2000**, *62*, 219–229.

(23) Eckert, H.; Wachs, I. E. *J. Phys. Chem.* **1989**, *93*, 6796–6805.

(24) Moffat, J. B. In *Metal Oxygen Clusters: The Surface and Catalytic Properties of Heteropoly Oxometalates*; Twigg, M. V., Spencer, M. S., Eds.; Kluwer Academic Publishers: New York, 2002.

(25) Rocchiccioli-Deltcheff, C.; Fournier, M.; Franck, R.; Thouvenot, R. *Inorg. Chem.* **1983**, *22*, 207–216.

(26) Fournier, M.; Aouissi, A.; Rocchiccioli-Deltcheff, C. *J. Chem. Soc., Chem. Commun.* **1994**, 307–308.

(27) Bardin, B. B.; Davis, R. J. *Appl. Catal., A* **1999**, *185*, 283–292.

(28) Busca, G. *J. Raman Spectrosc.* **2002**, *33*, 348–358.

(29) Busca, G. *Catal. Today* **1996**, *27*, 457–496.

(30) Caliman, E.; Dias, J. A.; Dias, S. C. L.; Prado, A. G. S. *Catal. Today* **2005**, *107−108*, 816–825.

(31) Deo, G.; Wachs, I. E. *J. Catal.* **1994**, *146*, 323–334.

(32) Kim, D. S.; Ostromecki, M.; Wachs, I. E. *J. Mol. Catal. A: Chem.* **1996**, *106*, 93–102.

(33) Brown, G. M.; Noe-Spirlet, M.-R.; Busing, W. R.; Levy, H. A. *Acta Crystallogr., Sect. B* **1977**, *33*, 1038–1046.

(34) Hardcastle, F. D.; Wachs, I. E. *J. Phys. Chem.* **1991**, *95*, 5031–5041.

(35) Gao, X.; Jehng, J.; Wachs, I. E. *J. Catal.* **2002**, *209*, 43–50.

(36) Rocchiccioli-Deltcheff, C.; Aouissi, A.; M. Bettahar, M.; Launay, S.; Fournier, M. *J. Catal.* **1996**, *164*, 16–27.

(37) Bielański, A.; Datka, J.; Gil, B.; Małecka-Lubańska, A.; Micek-Ilnicka, A. *Phys. Chem. Chem. Phys.* **1999**, *1*, 2355–2360.

(38) Burcham, L. J.; Briand, L. E.; Wachs, I. E. *Langmuir* **2001**, *17*, 6164–6174.

(39) Nakka, L.; Molinari, J. E.; Wachs, I. E. *J. Am. Chem. Soc.* **2009**, *131*, 15544–15554.

(40) Wang, C.; Cai, Y.; Wachs, I. E. *Langmuir* **1999**, *15*, 1223–1235.

(41) Wachs, I. E.; Jehng, J.; Ueda, W. *J. Phys. Chem. B* **2005**, *109*, 2275–2284.

(42) Kim, T. Fundamental structure-activity relationships for supported metal oxide catalysts. Ph.D. Dissertation, Lehigh University, Bethlehem, PA, 2007.

(43) Routray, K.; Briand, L. E.; Wachs, I. E. *J. Catal.* **2008**, *256*, 145–153.

(44) Kim, T.; Wachs, I. E. *J. Catal.* **2008**, *255*, 197–205.

(45) Highfield, J. G.; Moffat, J. B. *J. Catal.* **1985**, *95*, 108–119.

(46) Okuhara, T.; Tatematsu, S.; Lee, K. Y.; Misono, M. *Bull. Chem. Soc. Jpn.* **1989**, *62*, 717–723.

(47) Hirano, Y.; Inumaru, K.; Okuhara, T.; Misono, M. *Chem. Lett.* **1996**, *25*, 1111.

(48) Sorensen, C. M.; Weber, R. S. *J. Catal.* **1993**, *142*, 1–17.

(49) Badlani, M.; Wachs, I. E. *Catal. Lett.* **2001**, *75*, 137–149.

(50) Wachs, I. E.; Chen, Y.; Jehng, J.; Briand, L. E.; Tanaka, T. *Catal. Today* **2003**, *78*, 13–24.